



TEMPO Allegro: Liquid Catholyte Redoxmers for Nonaqueous Redox Flow Batteries

Journal:	<i>Journal of Materials Chemistry A</i>
Manuscript ID	TA-ART-05-2021-004297.R1
Article Type:	Paper
Date Submitted by the Author:	24-Jun-2021
Complete List of Authors:	ZHAO, YUYUE; Argonne National Laboratory, Chemical Sciences and Engineering Division Zhang, Jingjing; Argonne National Laboratory Agarwal, Garvit; Argonne National Laboratory, Materials Science Division Yu, Zhou; Argonne National Laboratory, MSD Corman, Rebecca ; University of Illinois at Urbana-Champaign Wang, Yilin; University of Illinois at Urbana-Champaign, Mechanical science and engineering Robertson, Lily ; Argonne National Laboratory, Chemical Sciences and Engineering Division Shi, Zhangxing; Argonne National Laboratory Doan, Hieu; Argonne National Laboratory, Material Science Division Ewoldt, Randy; University of Illinois at Urbana-Champaign Shkrob, Ilya; Argonne National Laboratory, Chemical Sciences and Engineering Surendran Assary, Rajeev; Argonne National Laboratory, Material Science Division Cheng, Lei; Argonne National Laboratory, Materials Science Division Srinivasan, Venkat; Argonne National Laboratory, Babinec, Susan; Argonne National Laboratory, Argonne Collaborative Center for Energy Storage Science Zhang, Lu; Argonne National Laboratory

TEMPO Allegro: Liquid Catholyte Redoxmers for Nonaqueous Redox Flow Batteries

Yuyue Zhao^{1,2,+}, Jingjing Zhang^{1,2,+}, Garvit Agarwal^{1,3}, Zhou Yu^{1,3}, Rebecca E. Corman^{1,4}, Yilin Wang^{1,4}, Lily A. Robertson^{1,2}, Zhangxing Shi², Hieu A. Doan^{1,3}, Randy H. Ewoldt^{1,4}, Ilya A. Shkrob^{1,2}, Rajeev S. Assary^{1,3}, Lei Cheng^{1,3}, Venkat Srinivasan^{1,5}, Susan J. Babinec⁵, and Lu Zhang^{1,2,*}

¹ Joint Center for Energy Storage Research, Argonne National Laboratory, Lemont, IL 60439, United States

² Chemical Sciences and Engineering Division, Argonne National Laboratory, Lemont, Illinois, 60439, United States

³ Material Science Division, Argonne National Laboratory, Lemont, Illinois, 60439, United States

⁴ Mechanical Science and Engineering, University of Illinois at Urbana–Champaign, Urbana, Illinois 61801, United States

⁵ Argonne Collaborative Center for Energy Storage Science, Argonne National Laboratory, Lemont, IL 60439, United States

Keywords: (TEMPO, liquid redoxmer, high concentration catholyte, nonaqueous flow battery)

Abstract:

Redoxmers are organic active molecules storing energy in redox flow batteries (RFBs). Liquid redoxmers represent an extreme scenario where maximum concentration may be achieved by minimizing supporting solvents, thus maximizing energy density of RFBs. Herein, a series of (2,2,6,6-tetramethylpiperidin-1-yl)oxyl (TEMPO)-based high potential (catholyte) liquid redoxmers, TEMPO-EG1, TEMPO-EG2, and TEMPO-EG3, were developed by incorporating polyethylene glycol (PEG) chains. Such modifications not only afford dramatic physical changes from solid to liquid and full miscibility in acetonitrile, but also impact the redox behavior. DFT calculation indicate that the incorporated PEG chains impact the charge distribution, which may account for the electrochemical changes. Importantly, compared to our previous liquid catholytes, the new redoxmers exhibit lower viscosity, which is desired for enhancing high concentration cycling performance. By using a hybrid flow cell, TEMPO-EG1 demonstrated more than 70% capacity retention over 100 cycles at 0.1 M and 66% capacity retention at 0.5 M, affording excellent cyclability at various concentrations. The study exemplifies how molecular engineering tuned the rheological properties of redoxmers, such

as viscosity, to improve high concentration cycling of RFBs, which may represent a promising avenue to a high energy density and low-cost flow battery system.

Introduction:

With soaring demand of carbon free electricity in our ever-growing society, sustainable energy resources, such as wind and solar, have become the fastest growing approach to electricity production.¹⁻⁴ However, their intermittent nature often leads to mismatches of supply and demand, posing challenges for grid-scale integration.⁵⁻⁶ Incorporating stationary energy storage into the grid is a promising solution to this issue as it enables the time domain, and smooths out the discrepancy of such mismatches. Given the large scale required for stationary storage, redox flow battery (RFB) technology is an emerging candidate due to its low cost and independence from critical materials in its supply chain. Different from traditional batteries, active materials are contained in the liquid electrolyte solutions, circulating through the positive and negative electrode compartments of the cell for energy conversion. The flowable nature of RFBs enables several features that are attractive for stationary energy storage, such as independent scaled power and energy, ease of scale-up and low-cost optimization.⁷⁻⁹

Depending on the solvents used, RFBs can be divided into two distinct categories of aqueous and nonaqueous based chemistries. While aqueous RFBs have shown stable performance and pre-commercial scale demonstrations, the intrinsic limitation from water electrolysis constrains the cell voltages and decreases energy density, resulting in increased system level cost, which hinders further market penetration. Nonaqueous RFBs (NRFBs) use organic solvents and provide an alternative solution due to a wider electrochemical window (>2 V) and a promise of enhanced energy density. The much improved electrochemical window stimulated significant material developments, and some examples include inorganic materials (sulfur and iodine species),¹⁰⁻¹¹ redox-active polymers,¹²⁻¹³ and organometallic compounds¹⁴⁻¹⁵ as well as hybrid designs such as semi-solid¹⁶⁻¹⁷ and redox-targeting flow batteries¹⁸⁻¹⁹. Among these materials, redox-active organic molecules (redoxmers) draw significant attention as they can be feasibly modified with tuneable properties at a low cost, making them ideal for constructing high energy density NRFBs.²⁰⁻²³

Besides tuning redox potentials to increase cell voltage, increasing solubility of redoxmers is an important approach for increasing energy density of NRFBs as effective redoxmer concentration determines how much electricity can be stored.²⁴ The ultimate goal is to achieve the maximum solubility without compromising viscosity and conductivity. Creating an intramolecular dipole moment is a proven approach for designing soluble redoxmers since

polar molecules are typically more soluble in polar electrolytes (*like dissolves like*). Our earlier studies indicate decreasing the molecular symmetry led to increased dipole moment, which improved solubility, but often at a price of decreasing stability due to uneven distribution of spin and charge density in a charged molecule.²⁵⁻²⁷ This trade-off can be managed with carefully introduced polar solubilizing groups, which increases solubility via creating local polarity without interfering with the balanced redox core structures. For instance, ANL-8 (Figure 1) was designed based on a stable redox core of 2,5-di-*tert*-butyl-1,4-dimethoxybenzene (DDB) with non-symmetric introduction of a short polyethylene glycol (PEG) chain. While DDB has limited solubility in organic solvents, ANL-8 is a borderline room temperature liquid that is fully miscible with acetonitrile (CH₃CN).²⁸ This dramatic change not only increases solubility but also enables the possibility of approaching theoretical capacity by using neat liquid redoxmers as supporting solvents or co-solvents. Several attempts have been conducted towards this extreme scenario.²³ However, when concentrated redoxmers are cycled in RFB cells, the increased viscosity becomes a major obstacle that leads to deteriorated cycling performance. For instance, when coupled with 2,1,3-benzothiadiazole, ANL-8 delivered excellent cycling performance at 0.1 M but showed poor material utilization at 0.5 M and 1.0 M due to polarization in the cell that was caused by high viscosity.²³ Limiting the viscosity over increased concentrations is a key challenge for high-concentration cycling and redoxmer design,²⁹⁻³⁰ and developing redoxmers with intrinsically low viscosity is paramount to mitigate such issues.

Herein, a series of redoxmers, TEMPO-EG1, TEMPO-EG2, and TEMPO-EG3, have been designed by introducing PEG chains of different lengths into a nitroxyl radical (2,2,6,6-tetramethylpiperidin-1-yl)oxyl (TEMPO) shown in **Figure 1**. As expected, the introduced PEG chains significantly impact the physical properties of the synthesized redoxmers. All three redoxmers become liquid at room temperature and are miscible with CH₃CN. Importantly, these new liquid redoxmers exhibit much lower viscosity compared to ANL-8 and deliver excellent cycling performance in flow cells.

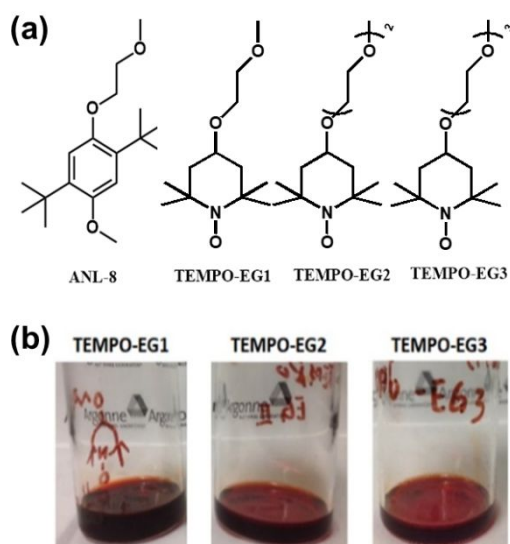


Figure 1. Structures and images of liquid redoxmers: (a) The chemical structures of liquid redoxmers, (b) the digital images of home-made liquid redoxmers with low viscosity

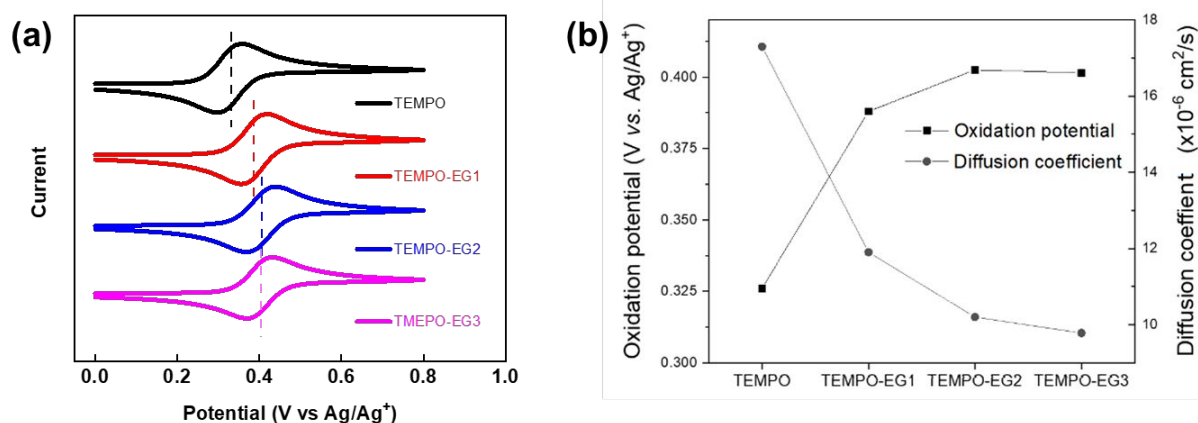


Figure 2. (a) Cyclic voltammograms of 10 mM TEMPO-based redoxmers in CH_3CN containing 0.5 M LiTFSI as the supporting electrolyte. The scan rate was 100 mV s^{-1} , and the current was normalized to facilitate comparison. (b) The oxidation potentials and diffusion coefficients of these four redoxmers.

Results and discussion:

The TEMPO-based redoxmers were synthesized using a simple Williamson ether coupling reaction of 4-hydroxy-TEMPO and the corresponding tosylated ether chain of desired PEG length. Details can be found in the experimental section of the Supporting Information. The

design of incorporating PEG chains followed our previous liquid redoxmer design of the ANL-8 series, and this simple modification indeed turned solid TEMPO into liquids as shown in Figure 1, which are also miscible with CH₃CN. As shown in Figure 2, all TEMPO-based redoxmers are electrochemically reversible in a supporting electrolyte of 0.5 M lithium bis(trifluoromethanesulfonyl)imide (LiTFSI) in CH₃CN, and the redox potentials slightly increase with the incorporated chains. For instance, compared to the halfwave potential ($E_{1/2}$) of TEMPO at 0.33 V vs. Ag/Ag⁺, the $E_{1/2}$ of TEMPO-EG1 positively shifts by ~60 mV to 0.39 V vs. Ag/Ag⁺. As the PEG chain grows, the increase continues but slows down to 0.40 V for TEMPO-EG2. For TEMPO-EG3, the potential does not change further. Such changes are not observed in the ANL-8 series where the redox potentials stay the same with or without incorporated PEG chains.²⁸ We speculate that the difference may stem from the perturbation of the PEG chains to the electronic energy of TEMPO.

Diffusion coefficients were also determined (for diffusion measurement procedure, see the Supporting Information). As shown in **Figure 2b**, as the molecular size increases, the diffusivity decreases from $17.3 \times 10^{-6} \text{ cm}^2 \text{ s}^{-1}$ for TEMPO to $11.9 \times 10^{-6} \text{ cm}^2 \text{ s}^{-1}$ for TEMPO-EG1 to $10.2 \times 10^{-6} \text{ cm}^2 \text{ s}^{-1}$ and $9.8 \times 10^{-6} \text{ cm}^2 \text{ s}^{-1}$ for TEMPO-EG2 and -EG3, respectively (see Table S1) The decrease in the diffusivity is not inversely proportional to the increase in the chain length, implying folded conformation for the chains. Indeed, it is well known that polyether chains strongly coordinate Li⁺ cations in electrolyte through their oxygen atoms.

For liquid redoxmers, a critical property is viscosity, which is directly associated with high capacity cycling. Viscosity measurements were performed using a microfluidic viscometer m-VROC (RheoSense, Inc.).²⁹ The fluid sample is pushed by a syringe pump into a rectangular microchannel with pressure measuring chip, where the viscosity is calculated by measuring flow rate and pressure drop. Figure 3 shows the dynamic viscosity of the liquid redoxmers for shear rates over one order of magnitude. All redoxmers exhibit Newtonian behavior as their viscosities do not significantly change with shear rate. The viscosity values can be obtained

from a Newtonian fit. TEMPO-EG1 and -EG2 show nearly identical viscosities, 10.2 and 10.9 mPa.s respectively, while TEMPO-EG3 approximately double at 21.3 mPa.s. While the prolonged PEG chain dramatically increases the viscosity, TEMPO-EG1 and TEMPO-EG2 show much lower viscosity compared to ANL-8 (23.4 mPa · s),²⁸ which is highly desired for improving cycling performance of RFBs.

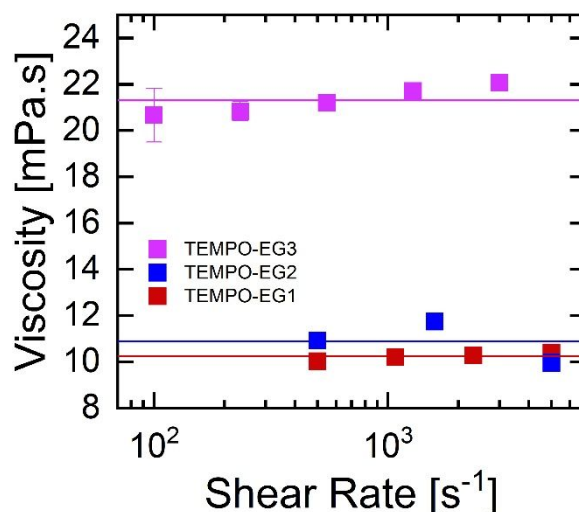


Figure 3. Viscosity of neat liquid TEMPO redoxmers vs. shear rate.

Density functional computations of solvated molecules were conducted to explore the effect of chemical modifications on property changes. **Figure 3**, Figure S5, and **Table 1** summarize the selected computed results such as frontier orbitals, $E_{1/2}$, and charge on certain atoms. Based on the highest occupied molecular orbital (HOMO) and lowest unoccupied molecular orbital (LUMO) profiles, the incorporation of PEG chains does not dramatically change the electron density distribution, which explains the preserved electrochemical reversibility. However, the modification decreased HOMO energies in the radical, which accounts for the increased redox potentials. The computed half-wave potentials $E_{1/2}$ are consistent with the experimental trends (Table 1, Table S2 and Table S3). The charge distribution in the molecules (Figure S5) indicates that addition of the ether chain decreases the charge on the nitrogen atom and increases the charge on the oxygen atom in the nitroxyl group. Such changes lead to increased redox potentials as removing an electron from the nitrogen atom

becomes less favorable thermodynamically. Qualitatively this effect can be understood as the increased strain in the chair-like 6-atom ring of TEMPO as the bulky group substitutes the equatorial hydrogen in the ring. The resulting strain makes it more difficult for the molecule to accommodate the nitroxyl group in either state of charge, resulting in a higher oxidation potential.

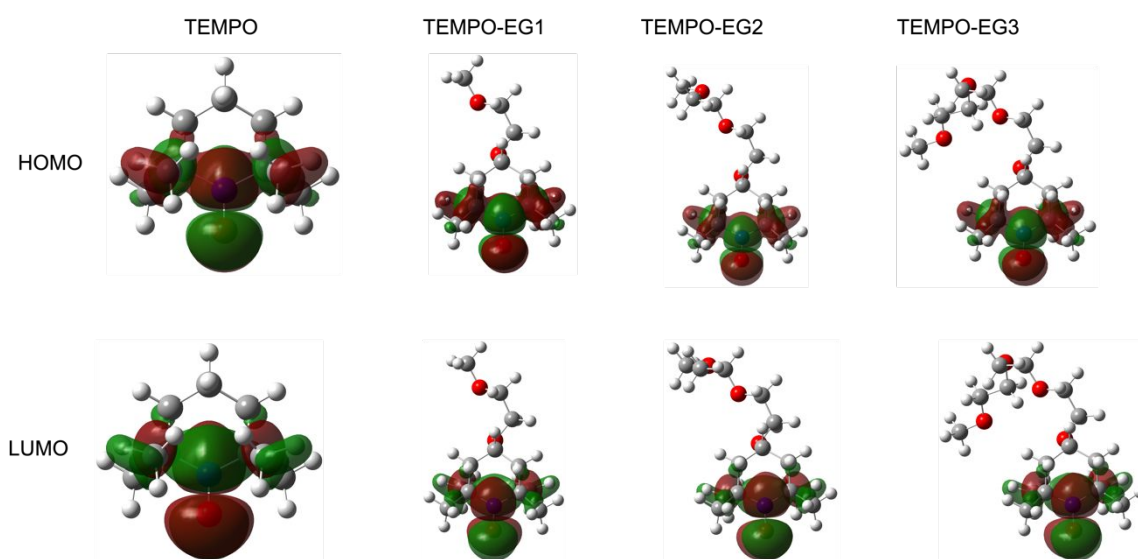


Figure 4. The HOMO and LUMO isosurfaces for TEMPO-based redoxmers.

Table 1. The computed HOMO energies, oxidation potential (E_{ox}) and atomic polar tensor (APT) charges on the nitrogen atom in TEMPO-based redoxmers.

	TEMPO	TEMPO-EG1	TEMPO-EG2	TEMPO-EG3
HOMO (eV)	-7.431	-8.439	-8.440	-8.443
E_{ox} (V, Ag/Ag ⁺)	0.163	0.232	0.243	0.247
Charge on N (e)	-0.13	-0.12	-0.11	-0.12

Symmetric cycling using a customized H-cell was used to evaluate the electrochemical cycling stability of redoxmers. TEMPO-EG1 was chosen for this test due to its combination of fast diffusivity, lowest molecular weight, high oxidation potential, and low viscosity. **Figure 5a**

shows the capacity retention profile of a symmetric H-cell containing 5 mM TEMPO-EG1 in 0.5 M LiTFSI in CH₃CN. Details of the cycling condition can be found in supporting information. At a cycling current of 5 mA, TEMPO-EG1 delivered an excellent capacity retention of 84% over 100 cycles. Cyclic voltammograms of the working chamber electrolyte obtained before and after cycling are shown in **Figure 5b**. While reduced peak current is observed, no shifts of the redox signals are seen, suggesting minimal side reactions and excellent stability of TEMPO-EG1. The reduced peak current may be related to possible crossover of redoxmers in the H-cell setup. As the redoxmer mass transfer may fluctuate in the static H cells over the cycling courses, the coulombic efficiency value may fluctuate as well, which may lead to values higher than 100% as observed in Figure 5a.

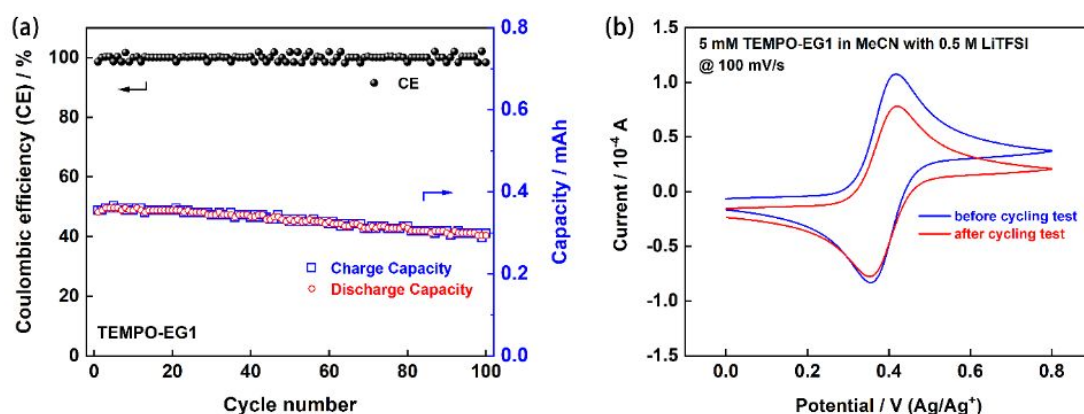


Figure 5. (a) Capacity retention profile for cycling of 5 mM TEMPO-EG1 in 0.5 M LiTFSI/CH₃CN at 5 mA; (b) CVs of the working chamber solution before and after cycling at 100 mV/s.

Next, a hybrid flow cell was adapted to characterize the cycling performance of TEMPO-EG1 at higher concentrations. In a hybrid flow cell, a lithium-graphite hybrid anode is coupled with the liquid catholyte (details can be found in the Supporting Information). This configuration allows full utilization of the high redox potentials of catholyte redoxmers and mitigates crossover issues, could lead to a high energy density and a low system-level cost.³¹ To accommodate Li metal, a carbonate-based electrolyte of 0.5 M LiTFSI in a 4:1:5 (by weight)

mixture of ethylene carbonate (EC), propylene carbonate (PC), and ethyl methyl carbonate (EMC) is used. Fluoroethylene carbonate (FEC) is added in 15 wt% to the electrolytes to improve interfacial stability. This additive is known to form robust passivation layers on the lithium-graphite, lithium metal, and lithiated silica electrodes in lithium-ion batteries.³²

As shown in Figure S3, TEMPO-based redoxmers exhibit reversible redox behavior in this electrolyte, and a positive shift of 60 mV (from ~ 3.54 V for TEMPO to 3.60 V for TEMPO-EG3 vs. Li/Li^+) was observed as the chain length increased. In this electrolyte, too, the redoxmer became less diffusive as the chain length increased (Figure S4).

Figures 6a, 6b and 6c summarize the performance of the hybrid flow cell containing 0.1 M TEMPO-EG1 and cycled at different constant current densities. As shown in the voltage-capacity profiles (**Figure 6a**), TEMPO-EG1 has a smooth charging plateau at ~ 3.7 - 3.8 V and a discharging plateau at ~ 3.4 - 3.2 V at 4 mA cm^{-2} , consistent with the redox potential observed in the CV measurements. As the current density increased, the gaps between charging and discharging plateaus became larger due to the increased overpotential. As a result, the discharge capacities decreased. This change is also seen in the efficiency profiles shown in **Figure 6b**. Among other changes, the Coulombic efficiency (CE) also slightly increased, while the voltage efficiency (VE) and energy efficiency (EE) both decreased. The CE at 4 mA cm^{-2} was 98.1%, and it gradually increased to 99.5% at 12 mA cm^{-2} , indicating low self-discharge and stable solid electrolyte interphase. On the other hand, VE and EE efficiencies decreased from 92.2% and 90.4% at 4 mA cm^{-2} to 75.1% and 74.7% at 12 mA cm^{-2} , respectively, indicating greater electrode overpotentials at higher current density.³³⁻³⁴

Given these tradeoffs, the current density of 8 mA cm^{-2} was chosen for long term cycle stability testing. **Figure 6c** shows the capacity retention and efficiency profiles over 100 cycles. For the first 50 cycles, the capacity fade remained steady with only 6.3% capacity loss from 9.5 mAh to 8.9 mAh. However, the capacity loss accelerated for the next 50 cycles with 22.1% decrease

to 6.8 mAh. While CE remained above 99% during this test, VE and EE decreased from 82.8% and 81.8% in the first cycle to 75% and 75% in the 100th cycle, respectively.

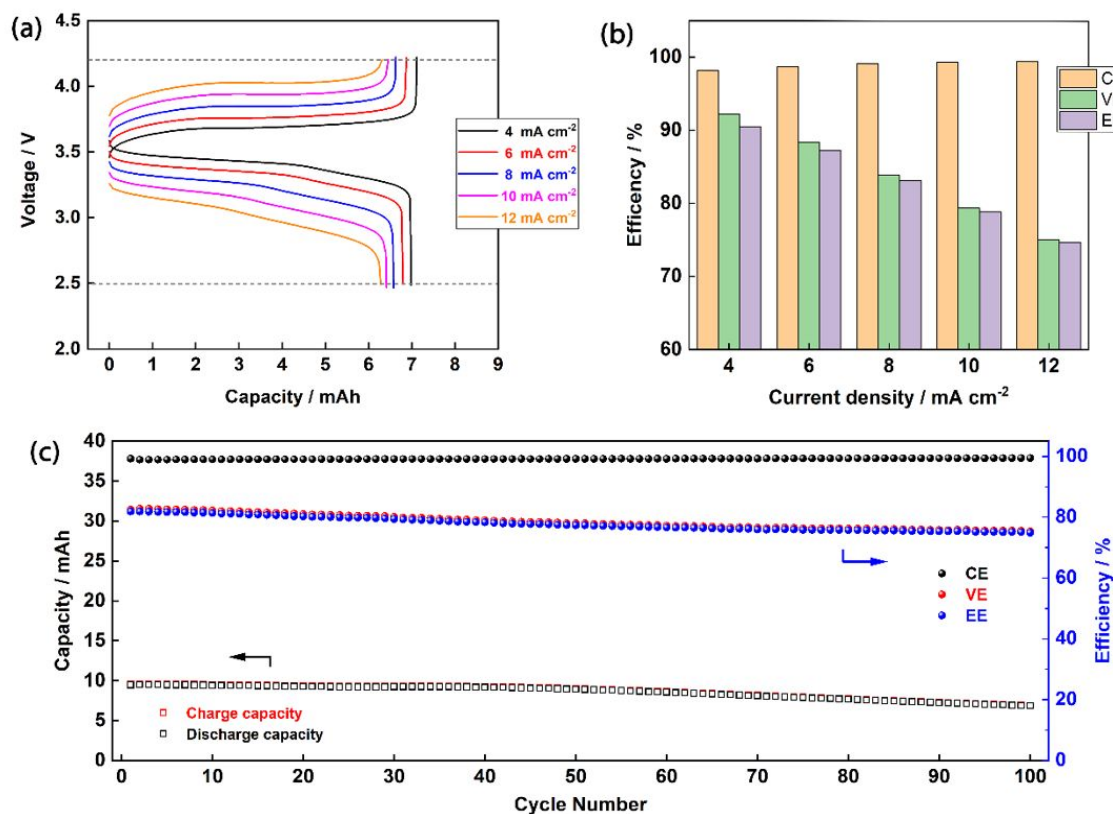


Figure 6. Cycling performance of the hybrid flow cell containing 0.1 M TEMPO-EG1 in the carbonate-based electrolyte. (a) Voltage-capacity profiles and (b) comparison of Coulombic efficiency (CE), voltage efficiency (VE), and energy efficiency (EE) over different current densities; (c) capacity retention and efficiency profiles over 100 cycles at the constant current density of 8 mA cm⁻².

Figure S6 shows the voltage-capacity profiles over 100 cycles. Initially, the discharge profiles consisted of two plateaus, one at ~3.4-3.2 V and another at ~3.2-3.0 V. As the cycling continued, the two plateaus merged into one. Such behavior may be due to a gradual transition from Li intercalation into graphite to Li plating on the polarized anode. As both Li metal and lithiated graphite are used in the anode, both processes can occur in concert (given the proximity of the

corresponding potentials), which accounts for the two discharging plateaus at the early stage of cycling. As cycling continues, more Li plating occurs, and the plateaus effectively merge into one. This interpretation is supported by a post-mortem examination of the cycled anode. Figure S7 shows the images of the harvested anode after 100 cycles, which indicate excessive Li metal deposition on the surface, suggesting that Li plating was the major reaction during late-stage cycling. When this anode was replaced with a fresh electrode, the stable cycling resumed (Figure S8). Minimal Li deposition was observed after 30 cycles, implying that no excessive Li deposition had occurred, which otherwise may contribute to the capacity decay.

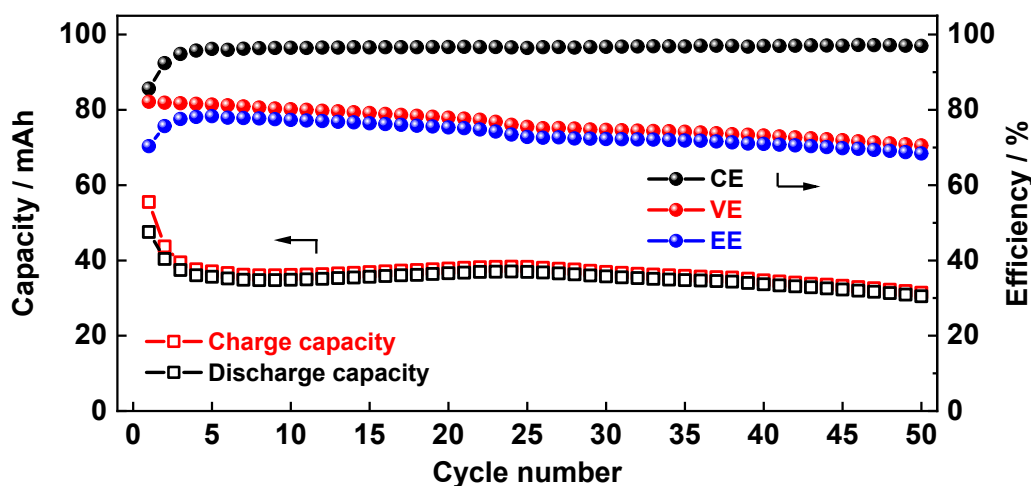


Figure 7. Capacity retention and efficiency profiles of the hybrid cell containing 0.5 M TEMPO-EG1 in the carbonate-based electrolyte cycled at a current density of 8 mA cm^{-2} over 50 cycles.

Given the improved viscosity, a higher concentration of 0.5 M TEMPO-EG1 was used in a hybrid flow cell cycled at the current density of 8 mA cm^{-2} (**Figure 7**). The electrode surface area was increased to 9 cm^2 to match the increased capacity. While the first three cycles indicated rapid capacity loss from 47 mAh to 37 mAh, the capacity retention from the 3rd to 50th cycle is good (39 mAh to 31 mAh), making the overall capacity retention 66%. For efficiencies, except for the first 3 cycles, CE maintained above 97%, while VE and EE were in the range of 80-70% and 76-67%, respectively, with a gradual decrease over time. While the

initial decrease of capacity should still be related to SEI-like reactions on anode, the following stabilized cycling performance indicates TEMPO-EG1 can deliver stable cycling even at a higher concentration.

Conclusion:

In this paper, a new series of catholyte redoxmers, TEMPO-EG1, EG-2, and EG-3, has been developed by introducing polar PEG chains into TEMPOs. Those modifications afford dramatic physical changes of the redoxmers from solid to liquid and full miscibility with organic solvents such as CH₃CN. Importantly, TEMPO-EG1 and -EG2 exhibit much improved viscosity at ~10 mPa · s, which is 50+% lower compared to the previous liquid redoxmer molecule, ANL-8. In addition, while the introduced PEG chains are not directly connected to the nitroxyl, such modifications strain TEMPO ring and affect the charge distribution, leading to redox potential increases. Due to the combination of fast diffusivity, high oxidation potential, and low viscosity, TEMPO-EG1 was extensively characterized for cycling stability using symmetric H-cell and hybrid flow cell designs and demonstrated stable cycling performance in both settings. In the symmetric H-cell, TEMPO-EG1 delivers a capacity retention of 83.8% over 100 cycles. When cycled in a hybrid flow cell, TEMPO-EG1 demonstrated more than 70% capacity retention over 100 cycles with an averaged Coulombic efficiency of 99%. The improved fluidity also enables improved cycling at higher concentration as TEMPO-EG1 delivers an overall capacity retention of 66% when cycled at 0.5 M. This study exemplifies using molecular engineering to tune the rheological properties of redoxmers, including viscosity, to improve high concentration cycling of NRFBs. By taking advantages of high capacity of liquid catholyte redoxmers and high cell voltage of hybrid cell configuration, a high energy density could be achieved, which may represent an alternative avenue to a low system-level cost.

Supporting Information

Supporting Information contains material synthesis,

Acknowledgements

This work is financially supported by Laboratory Directed Research and Development (LDRD) funding from Argonne National Laboratory, provided by the Director, Office of Science, of the U.S. Department of Energy under Contract No. DE-AC02-06CH11357. This research was also partially supported by the Joint Center for Energy Storage Research (JCESR), an Energy Innovation Hub funded by the U.S. Department of Energy, Office of Science, and Basic Energy Sciences. The submitted manuscript has been created by UChicago Argonne, LLC, Operator of Argonne National Laboratory (“Argonne”). Argonne, a U.S. Department of Energy Office of Science laboratory, is operated under Contract No. DE-AC02-06CH11357. We acknowledge a generous grant of computer time from the Argonne National Laboratory Computing Resource Center (Bebop). We also acknowledge the computational resources from Center for Nanoscale Materials, an Office of Science user facility, which was supported by the U.S. Department of Energy, Office of Science, Office of Basic Energy Sciences, under Contract No. DE-AC02-06CH11357. Yuyue Zhao and Jingjing Zhang contributed equally to this work.

Received: ((will be filled in by the editorial staff))

Revised: ((will be filled in by the editorial staff))

Published online: ((will be filled in by the editorial staff))

Reference:

1. Wang, W.; Luo, Q.; Li, B.; Wei, X.; Li, L.; Yang, Z., Recent Progress in Redox Flow Battery Research and Development. *Advanced Functional Materials* **2013**, *23* (8), 970-986.
2. Wei, X.; Pan, W.; Duan, W.; Hollas, A.; Yang, Z.; Li, B.; Nie, Z.; Liu, J.; Reed, D.; Wang, W.; Sprenkle, V., Materials and Systems for Organic Redox Flow Batteries: Status and Challenges. *ACS Energy Lett.* **2017**, *2* (9), 2187–2204.
3. Ding, Y.; Zhang, C.; Zhang, L.; Zhou, Y.; Yu, G., Molecular engineering of organic electroactive materials for redox flow batteries. *Chemical Society reviews* **2018**, *47* (1), 69-103.
4. Yang, Z.; Zhang, J.; Kintner-Meyer, M. C.; Lu, X.; Choi, D.; Lemmon, J. P.; Liu, J., Electrochemical energy storage for green grid. *Chemical reviews* **2011**, *111* (5), 3577-613.
5. Ding, C.; Zhang, H.; Li, X.; Liu, T.; Xing, F., Vanadium Flow Battery for Energy Storage: Prospects and Challenges. *The journal of physical chemistry letters* **2013**, *4* (8), 1281-94.
6. Lu, W.; Yuan, Z.; Zhao, Y.; Zhang, H.; Zhang, H.; Li, X., Porous membranes in secondary battery technologies. *Chemical Society reviews* **2017**, *46* (8), 2199-2236.
7. Kowalski, J. A.; Carney, T. J.; Huang, J.; Zhang, L.; Brushett, F. R., An investigation on the impact of halidization on substituted dimethoxybenzenes. *Electrochimica Acta* **2020**, *335*, 135580.

8. Zhang, L.; Zhang, J.; Wei, X.; Brushett, F. R.; Shkrob, I. A. In *Understanding Benzothiadiazole Based Anolyte Materials for Nonaqueous Redox Flow Cells*, Meeting Abstracts, The Electrochemical Society: 2019; pp 445-445.
9. Gür, T. M., Review of electrical energy storage technologies, materials and systems: challenges and prospects for large-scale grid storage. *Energy & Environmental Science* **2018**, *11* (10), 2696-2767.
10. Chen, H. N.; Lu, Y. C., A high-energy-density multiple redox semi-solid-liquid flow battery. *Adv. Energy Mater.* **2016**, *6*, 1502183.
11. Pratt, H. D.; Hudak, N. S.; Fang, X. K.; Anderson, T. M., A polyoxometalate flow battery. *J. Power Sources* **2013**, *236*, 259-264.
12. Nagarjuna, G.; Hui, J. S.; Cheng, K. J.; Lichtenstein, T.; Shen, M.; Moore, J. S.; Rodriguez-Lopez, J., Impact of Redox-Active Polymer Molecular Weight on the Electrochemical Properties and Transport Across Porous Separators in Nonaqueous Solvents. *J. Am. Chem. Soc.* **2014**, *136* (46), 16309-16316.
13. Montoto, E. C.; Nagarjuna, G.; Hui, J. S.; Burgess, M.; Sekerak, N. M.; Hernandez-Burgos, K.; Wei, T. S.; Kneer, M.; Grolman, J.; Cheng, K. J.; Lewis, J. A.; Moore, J. S.; Rodriguez-Lopez, J., Redox Active Colloids as Discrete Energy Storage Carriers. *J Am Chem Soc* **2016**, *138* (40), 13230-13237.
14. Sevov, C. S.; Fisher, S. L.; Thompson, L. T.; Sanford, M. S., Mechanism-Based Development of a Low-Potential, Soluble, and Cyclable Multielectron Anolyte for Nonaqueous Redox Flow Batteries. *J. Am. Chem. Soc.* **2016**, *138* (47), 15378-15384.
15. Ding, Y.; Zhao, Y.; Li, Y.; Goodenough, J. B.; Yu, G., A high-performance all-metalocene-based, non-aqueous redox flow battery. *Energy. Environ. Sci.* **2017**.
16. Duduta, M.; Ho, B.; Wood, V. C.; Limthongkul, P.; Brunini, V. E.; Carter, W. C.; Chiang, Y. M., Semi-Solid Lithium Rechargeable Flow Battery. *Adv. Energy Mater.* **2011**, *1* (4), 511-516.
17. Fan, F. Y.; Woodford, W. H.; Li, Z.; Baram, N.; Smith, K. C.; Helal, A.; McKinley, G. H.; Carter, W. C.; Chiang, Y. M., Polysulfide Flow Batteries Enabled by Percolating Nanoscale Conductor Networks. *Nano Lett* **2014**, *14* (4), 2210-2218.
18. Jia, C.; Pan, F. P.; Zhu, Y. G.; Huang, Q.; Lu, L.; Wang, Q., High-energy density nonaqueous all redox flow lithium battery enabled with a polymeric membrane. *Science Advances* **2015**, *1* (20), e1500886.
19. Huang, Q. Z.; Yang, J.; Ng, C. B.; Jia, C.; Wang, Q., A redox flow lithium battery based on the redox targeting reactions between LiFePO₄ and iodide. *Energy Environ Sci* **2016**, *9* (3), 917-921.
20. Gong, K.; Fang, Q.; Gu, S.; Li, S. F. Y.; Yan, Y., Nonaqueous redox-flow batteries: organic solvents, supporting electrolytes, and redox pairs. *Energy. Environ. Sci.* **2015**, *8* (12), 3515-3530.
21. Winsberg, J.; Hagemann, T.; Janoschka, T.; Hager, M. D.; Schubert, U. S., Redox-Flow Batteries: From Metals to Organic Redox-Active Materials. *Angew Chem Int Edit* **2017**, *56*, 686–711.
22. Park, M.; Ryu, J.; Wang, W.; Cho, J., Material design and engineering of next-generation flow-battery technologies. *Nat. Rev. Mater.* **2016**, Article number: 16080.
23. Duan, W.; Huang, J.; Kowalski, J. A.; Shkrob, I. A.; Vijayakumar, M.; Walter, E.; Pan, B.; Yang, Z.; Milshtein, J. D.; Li, B.; Liao, C.; Zhang, Z.; Wang, W.; Liu, J.; Moore, J. S.; Brushett, F. R.; Zhang, L.; Wei, X., “Wine-Dark Sea” in an Organic Flow Battery: Storing Negative Charge in 2,1,3-Benzothiadiazole Radicals Leads to Improved Cyclability. *ACS Energy Letters* **2017**, *2* (5), 1156-1161.
24. Huang, Q.; Wang, Q., Next-Generation, High-Energy-Density Redox Flow Batteries. *ChemPlusChem* **2014**, *80* (2), 312-322.

25. Zhang, Z.; Zhang, L.; Schlueter, J. A.; Redfern, P. C.; Curtiss, L.; Amine, K., Understanding the redox shuttle stability of 3,5-di-tert-butyl-1,2-dimethoxybenzene for overcharge protection of lithium-ion batteries. *Journal of Power Sources* **2010**, *195* (15), 4957-4962.
26. Zhang, L.; Zhang, Z.; Redfern, P. C.; Curtiss, L. A.; Amine, K., Molecular engineering towards safer lithium-ion batteries: a highly stable and compatible redox shuttle for overcharge protection. *Energy & Environmental Science* **2012**, *5* (8), 8204-8207.
27. Weng, W.; Huang, J.; Shkrob, I. A.; Zhang, L.; Zhang, Z., Redox Shuttles with Axisymmetric Scaffold for Overcharge Protection of Lithium-Ion Batteries. *Advanced Energy Materials* **2016**, *6* (19), 1600795.
28. Huang, J.; Cheng, L.; Assary, R. S.; Wang, P.; Xue, Z.; Burrell, A. K.; Curtiss, L. A.; Zhang, L., Liquid Catholyte Molecules for Nonaqueous Redox Flow Batteries. *Advanced Energy Materials* **2015**, *5* (6), n/a-n/a.
29. Wang, Y.; Kaur, A. P.; Attanayake, N. H.; Yu, Z.; Suduwella, T. M.; Cheng, L.; Odom, S. A.; Ewoldt, R. H., Viscous flow properties and hydrodynamic diameter of phenothiazine-based redox-active molecules in different supporting salt environments. *Physics of Fluids* **2020**, *32* (8), 083108.
30. Attanayake, N. H.; Liang, Z.; Wang, Y.; Kaur, A. P.; Parkin, S. R.; Mobley, J. K.; Ewoldt, R. H.; Landon, J.; Odom, S. A., Dual function organic active materials for nonaqueous redox flow batteries. *Materials Advances* **2021**.
31. Darling, R. M.; Gallagher, K. G.; Kowalski, J. A.; Ha, S.; Brushett, F. R., Pathways to low-cost electrochemical energy storage: a comparison of aqueous and nonaqueous flow batteries. *Energy & Environmental Science* **2014**, *7* (11), 3459-3477.
32. Wei, X.; Xu, W.; Vijayakumar, M.; Cosimbescu, L.; Liu, T.; Sprenkle, V.; Wang, W., TEMPO-based catholyte for high-energy density nonaqueous redox flow batteries. *Adv Mater* **2014**, *26* (45), 7649-53.
33. Zhao, Y.; Li, M.; Yuan, Z.; Li, X.; Zhang, H.; Vankelecom, I. F. J., Advanced Charged Sponge-Like Membrane with Ultrahigh Stability and Selectivity for Vanadium Flow Batteries. *Advanced Functional Materials* **2016**, *26* (2), 210-218.
34. Winsberg, J.; Janoschka, T.; Morgenstern, S.; Hagemann, T.; Muench, S.; Hauffman, G.; Gohy, J. F.; Hager, M. D.; Schubert, U. S., Poly(TEMPO)/Zinc Hybrid-Flow Battery: A Novel, "Green," High Voltage, and Safe Energy Storage System. *Adv Mater* **2016**, *28* (11), 2238-43.